Structures 78 (2025) 109374

Contents lists available at ScienceDirect

Structures

journal homepage: www.elsevier.com/locate/structures

# Fragility curves for the seismic vulnerability of a stock of Italian highway bridges

Pietro Crespi [a], Manuela Scamardo [a,*], Rocco Buoninconti [b]

[a] Architecture, Built Environment and Construction Engineering Dept., Politecnico di Milano, Milan, Italy
[b] ETS srl, Milan, Italy

ARTICLE INFO

*Keywords:*
Seismic vulnerability
Fragility curves
Modal pushover
Highway bridges
Risk index

ABSTRACT

The present study aims to analyze a stock of highway bridges of the Italian motorway network for the determination of analytical fragility curves, based on nonlinear modal pushover analyses. Fragility curves represent a valid and reliable tool for seismic risk evaluation and allow to correlate the probability of damage exceedance to the earthquake intensity, here represented through the peak ground acceleration. Fragility curves are fundamental in bridge management software to evaluate possible intervention scenarios and to schedule maintenance or retrofitting works by optimizing the economic resources. The obtained results showed a recurrent failure sequence: for increasing values of the peak ground acceleration, a shear failure of the pier is detected at first, followed by the bending failure of the base section of the pier and the unseating of the deck. Furthermore, the behavior in the transverse direction of the bridge results more critical, especially for long viaducts. The fragility curves were also compared with the ones presented in the scientific literature by other researchers for different bridge stocks. The curves result in agreement with the ones determined by other researchers with nonlinear static analyses, while they result conservative with respect to those determined with nonlinear time history analyses.

## 1. Introduction

The safety level of a structure against the expected earthquake can be determined with a seismic vulnerability analysis, which can be interpreted as a comparison between the bearing capacity of the structure and the seismic demand of the site. In the last decades, more and more attention has been devoted to the seismic problem by the scientific community [1,2]. Earthquakes happen without clear notice and could not be forecasted, resulting in inconveniences and unpredictability. However, the earthquakes happened in the past allowed the study of this phenomenon giving the possibility to cumulate knowledge on the subject and strategies to limit the undesired effects [3].

A lot of Italian structures are close to the end of their service life and requires extensive maintenance, repairing or retrofitting works [4,5]. A large part of this stock of structures is represented by bridges, viaducts, overpasses or underpasses of the national highway network. Although they were designed for a long service life [6], these structures are commonly subjected to damages due to increased amount of traffic [6–8], augmented traffic loads [9,10], severe environmental conditions [11,12], and accidental actions [13,14] that could significantly reduce their performances. In recent years, the Italian Civil Protection agency asked to the highway management companies to produce the results of nonlinear seismic assessments of each asset in their portfolios for emergency planning and prioritization of the maintenance works [15–17].

With this in mind, the present work is focused on the seismic vulnerability analysis of a stock of reinforced concrete (RC) viaducts of the northern Italy, managed by a highway authority. Analytical fragility curves have been determined for a stock of 1182 RC viaducts by correlating the probability of damage exceedance with the earthquake intensity, as measured by the peak ground acceleration (PGA). The curves were defined on the basis of the results of seismic safety assessments obtained from non-linear modal pushover analyses carried out at the request of the Italian Civil Protection agency.

Differently from many other works, here the fragility curves are not related to individual viaducts but to a portfolio of bridges, one of the largest studied in literature (see also Section 5), considering, globally or in subgroups, the variability of the configurations of the structures.

The obtained fragility curves are useful for large-scale application, at the level of the infrastructure network. Indeed, they represent a powerful tool for highways authorities in their bridge management strategies for the following reasons: (i) they allow the quantification of

* Corresponding author.
*E-mail address:* manuela.scamardo@polimi.it (M. Scamardo).

https://doi.org/10.1016/j.istruc.2025.109374
Received 17 January 2025; Received in revised form 22 May 2025; Accepted 4 June 2025
Available online 8 June 2025

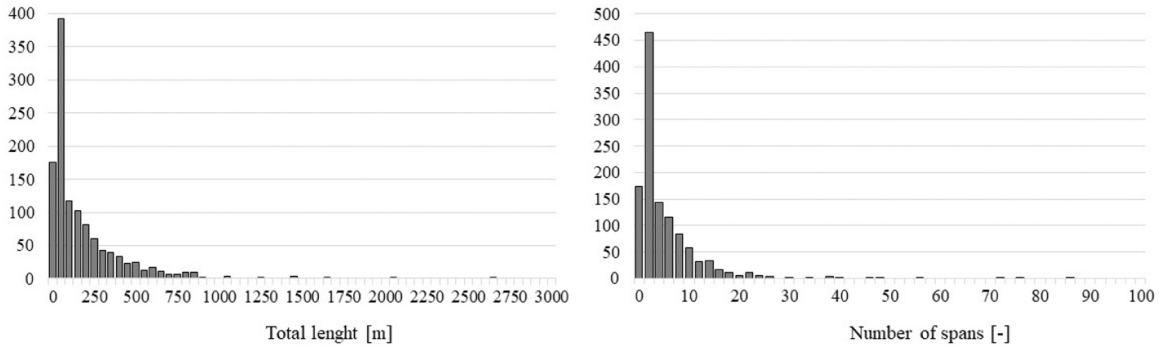


**Fig. 1.** Length of the bridge (a) and number of spans (b) distribution.

the overall risk associated with the bridge infrastructure, identifying likely failure types and vulnerable bridges; (ii) they allow to optimize the maintenance and inspection programs, with the consequent prioritization of the interventions on bridges that contribute most significantly to the overall risk, and a more efficient allocation of economic resources; (iii) they can guide long-term infrastructure investment decisions, ensuring that new bridge designs and replacements incorporate measures to reduce fragility and enhance resilience against identified hazards.

## 2. Database description

A total of 1182 RC bridges have been analyzed in this study, corresponding to about 90 % of the stock of viaducts hold by a company in charge of managing their continuous monitoring and maintenance. Each bridge of the stock is identified with an acronym (ID code). The results of the seismic vulnerability assessment of the bridges have been stored in a database controlled by the company (hereafter referred to as the SIOS database).

For each bridge considered in this work, the following data have been extracted from the company database: ID code of the bridge, type of structure, number of spans, total length of the bridge, peak ground acceleration ($PGA_D$) value of the site prescribed by the design code [4], maximum peak ground acceleration values bearable by the structure ($PGA_C$) against three failure modes (i.e., bending failure of a pier, shear failure of a pier, unseating of the deck) for both the longitudinal and transverse direction of the bridge, return period ($T_{RD}$) of the earthquake prescribed by the design code, maximum return periods of the earthquake leading to the failure of the structure ($T_{RC}$) for the three considered failure modes, and the risk indices (RI) of the structure expressed as a function of both PGA and $T_R$ for both the principal directions of the bridge (longitudinal and transverse). The procedure followed for the determination of the capacity of the bridge ($PGA_C$, $T_{RC}$) and the risk indices are described in Section 3.1.

From the collected data, it results that the number of spans of the bridge's database ranges between 1 and 87, while the length of the bridges ranges between 7 m and 2672 m, with the distribution described in Fig. 1.

In Fig. 1a, the total lengths of bridges are grouped in classes of 50 m each. The class with the highest number of bridges (392) is the one with a total length between 50 and 99 m, which represents 33 % of all bridges. The 15 % (176) is between 7 m (minimum value) and 49 m, while the 10 % (117) falls between 100 m and 149 m. In general, the majority of the bridge lengths is below 500 m, while the maximum bridge length is 2672 m.

In Fig. 1b, the numbers of spans are grouped in classes of 2 spans each. The class with the highest number of bridges (466) is the one with a number of spans between 3 and 4, which represents 39 % of all bridges. The 12 % (143) is between 5 and 6, while the 10 % (116) falls between 7 and 8. It is important to highlight the presence in the SIOS database of 112 short bridges (9 %), with only one span. In general, most of the bridges have a number of spans below 20, while the rest is unevenly distributed among the other classes, with a maximum value of 87 spans for the longest bridge. In the following, specific fragility curves will be developed for the whole stock of bridges and for three different ranges of length and number of spans of the bridges. This represents the simplest way of grouping the structures by filtering the bridge database, according to the peculiarity of the SIOS database. However, other ways of grouping viaducts could be considered in the future (e.g. structure type, pier cross-section, span configuration, bearing type).

## 3. Definition of the fragility curves

Fragility curves describe the probability of a structure to reach or exceed a specific damage state (DS) under earthquake excitation. They establish a relationship between a measure of the intensity of the seismic action IM and the probability of the structure of being damaged beyond a specific level of damage $DS_k$. Several options are available for the measure of IM as, for instance, peak ground acceleration, peak ground velocity, root mean square velocity, spectral acceleration at the natural period of the bridge [18,19]. In this study, the PGA has been chosen as intensity measure to make possible the comparison with other works previously presented in the scientific literature [20–31]. As damage level, the significant damage limit state [32] or life safety limit state [4] are considered.

Analytically, by assuming a lognormal cumulative distribution function [33], this statement can be expressed as follows:

$$P(DS \geq DS_k|IM) = \Phi\left(\frac{\ln IM - \mu_{DS|IM}}{\beta}\right) \quad (1)$$

where $\Phi$ represents the standard normal cumulative distribution function, $\mu_{DS|IM}$ is the lognormal mean of the DS conditioned on IM, and $\beta$ is the lognormal standard deviation of DS|IM.

The lognormal distribution is commonly adopted in seismic vulnerability studies because: (i) it fits well the distribution of structural failure data [34–36], (ii) it has zero probability density below zero IM, and (iii) it is fully characterized by the first and second moments of the distribution.

Fragility curves can be obtained in different ways: (i) from expert opinion (expert judgement fragility curves), (ii) from statistical processing of post-earthquake survey data (empirical fragility curves), or (iii) from analytical or numerical evaluations (analytical fragility curves).

In the present work, analytical fragility curves will be determined for a stock of existing bridges by defining the lognormal cumulative distribution function F(PGA) as:

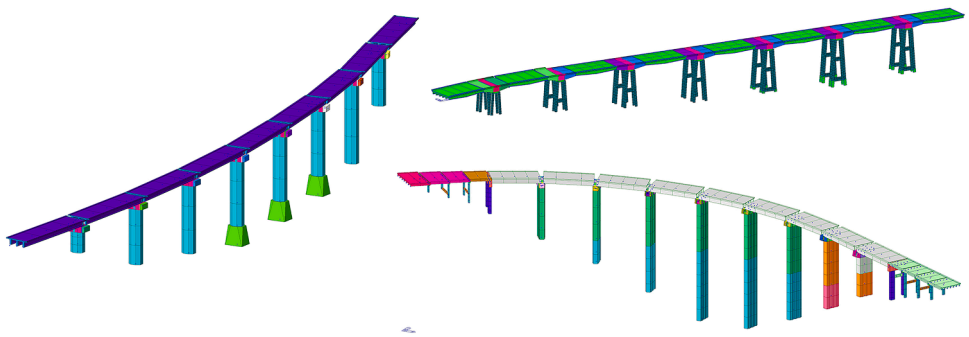

**Fig. 2.** – Examples of FE models of highway bridges of the considered stock.

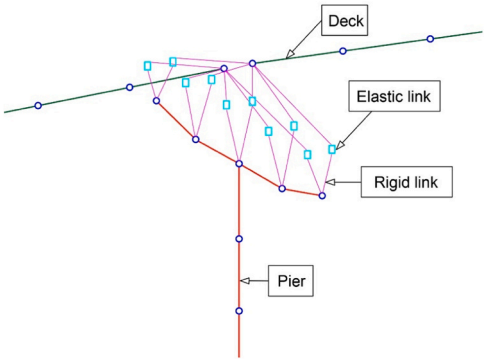


**Fig. 3.** – Wireframe view of a part of a bridge model.

$$F(PGA) = \Phi\left[\frac{1}{\beta}\ln\left(\frac{PGA}{x_m}\right)\right] \quad (2)$$

where $x_m$ is the median value of the damage state ($DS_k$) capacity, expressed in terms of acceleration, and β is the logarithmic standard deviation [37,38].

The required parameters of the lognormal curve are obtained as follows [34]:

$$\mu = \frac{1}{N}\sum_{i=1}^{N}\ln PGA_i \quad (3)$$

$$x_m = e^{\mu} \quad (4)$$

$$\beta = \sqrt{\frac{1}{N-1}\sum_{i=1}^{N}(\ln PGA_i - \mu)^2} \quad (5)$$

where $PGA_i$ is the median IM leading to the reaching of the damage state $DS_k$ and N is the number of considered bridges.

### 3.1. Seismic vulnerability assessment procedure

For the evaluation of the seismic vulnerability, all the 1182 RC highway bridges of the considered stock have been modeled in the finite element (FE) software Midas Civil (Fig. 2) to perform nonlinear static analyses (NLSA) and obtain their capacity curves. NLSA allows the modelling of the nonlinear behavior of the structural members and the determination of the capacity of the structure in a simple and fairly rapid way. Although the use of nonlinear time history analysis could have provided more detailed results, its computational cost is too high for such a large number of bridges. The structures have been modeled using beam elements and elastic/rigid links (Fig. 3). The bending and shear nonlinear behavior of piers and bearings has been modeled with proper plastic hinges as described in detail in [39,40]. The obtained results (e.g., capacity curves, stresses, displacements) have been imported into a custom software specifically written in Matlab (called MPA_CISE), which automatically performs the modal pushover analyses (MPA) [41–44] in order to find the performance point (PP) of the structure (i.e., the intersection between the capacity and demand curves, according to the capacity spectrum method [3,45], following the procedure described in ATC-40 [46]) for each significant vibration mode, and [4,15] for the two main directions (longitudinal X and transverse Y). The PP gives the response of the structure subjected to the expected seismic event.

For each modelled viaduct, the MPA_CISE software performs a great number of iterations in order to find the PP of the structure by intersecting each capacity curve with a progressively increasing design spectrum (controlled by increasing the PGA), obtaining as a result the PGA associated to the considered damage state (i.e., when a failure of a member happens for the first time), in this case assumed as the significant damage limit state [32] or life safety limit state [4]. Following the modal pushover analysis approach [41,42], this process implies the consideration of all the significant vibration mode shapes of the bridge (at least the ones with a participant mass greater than 2 %) and the combination of the results with the complete quadratic combination (CQC) or the square root of the sum of the squares (SRSS) combination rules, for the two principal directions of the viaduct (i.e., longitudinal and transverse). At the end of this iterative procedure, the capacity of the structure is known in terms of maximum $PGA_C$ bearable by the structure, and this result can be compared with the corresponding $PGA_D$ prescribed by the code for the considered site. The ratio between the two PGAs represents the so-called risk index ($RI = PGA_C/PGA_D$) as defined by the Italian design code [4,15]. The limit safety condition of the structure is defined by RI equal to 1 and the lower is RI, the higher is the probability of collapse of the structure. Further details about the FE modelling of bridges, implementation of the procedure, and validation of the results can be found in [39,40,47].

The modal pushover analyses results obtained for each structure are saved automatically by the MPA_CISE software in text files and stored in the SIOS database, hosted by the company in charge of managing the network of the considered highway bridges.

These results are then used as input in the FC_Gen (Fragility Curves Generator) Matlab software, specifically developed by the authors to determine and plot the fragility curves of the bridges stock. This code reads and extrapolates the previously evaluated critical $PGA_C$ of the bridges and determines the corresponding fragility curve, by grouping the results with respect to the failure mode (bending, shear, and unseating), loading direction (longitudinal or transverse), and number of considered bridges (e.g., whole stock, bridges pertaining to different highway authorities, length of the bridge). Therefore, the obtained fragility curves should be interpreted as bridge class fragility curves and not as individual bridge fragility curves. Furthermore, having used the smoothed response spectrum prescribed by the code in the modal pushover analyses, the record-to-record variability is not accounted.

It should be also highlighted that the considered fragility curves were obtained from the results of vulnerability analyses performed on the

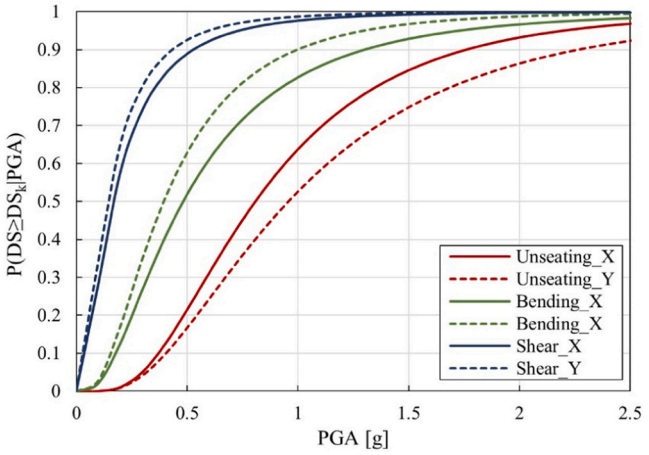


**Fig. 4.** – Fragility curves of the whole SIOS database.

**Table 1**
– Parameters of the fragility curves of the whole SIOS database.

| | X | | Y | |
|---|---|---|---|---|
| Verification | $x_m$ [g] | β | $x_m$ [g] | β |
| Unseating | 0.8081 | 0.6069 | 0.9572 | 0.6720 |
| Bending | 0.4822 | 0.7735 | 0.3948 | 0.7226 |
| Shear | 0.1666 | 0.8997 | 0.1415 | 0.8735 |

**Table 2 –**
Parameters of the fragility curves for total length grouping in longitudinal (X) direction.

| | Short | | Medium | | Long | |
|---|---|---|---|---|---|---|
| Verification | $x_m$ [g] | β | $x_m$ [g] | β | $x_m$ [g] | β |
| Unseating | 0.7226 | 0.5763 | 0.7641 | 0.5401 | 0.8900 | 0.6496 |
| Bending | 0.7986 | 0.8389 | 0.4089 | 0.6751 | 0.3991 | 0.6546 |
| Shear | 0.2480 | 1.1159 | 0.1366 | 0.7721 | 0.1503 | 0.7545 |

**Table 3 –**
Parameters of the fragility curves for total length grouping in transverse (Y) direction.

| | Short | | Medium | | Long | |
|---|---|---|---|---|---|---|
| Verification | $x_m$ [g] | β | $x_m$ [g] | β | $x_m$ [g] | β |
| Unseating | 0.9302 | 0.7093 | 0.9560 | 0.6039 | 0.9725 | 0.6952 |
| Bending | 0.3732 | 0.8844 | 0.4366 | 0.7194 | 0.3821 | 0.6045 |
| Shear | 0.1131 | 0.9424 | 0.1604 | 0.8953 | 0.1487 | 0.7920 |

initial bridge configuration, disregarding the influence of the damage evolution over time caused by factors such as ageing, corrosion, traffic loads and maintenance activities on the performance of the bridges. As demonstrated by other works on the subject [5,11,40], it has been shown that, as expected, corrosion leads to an increase in the vulnerability of bridges (i.e. increase of exceeding probability for a certain PGA) as well as an increase in the corresponding standard deviation. Conversely, the implementation of potential upgrading interventions on the bridges of the aforementioned stock during scheduled maintenance activities follow in opposite effects. Presently, the availability of these results is restricted to a modest subset of bridge structures [48]. Consequently, the incorporation of these results into fragility curves remains a subject of ongoing evaluation.

### 3.2. *Fragility curves of the whole bridges stock*

Following the presented procedure, the fragility curves related to all the bridges of the SIOS database have been obtained (Fig. 4) with regard to the three most important failure modes, i.e., bending or shear failure of the piers, and unseating failure of the deck, for both the longitudinal (X, solid lines) and transverse (Y, dashed lines) direction. The main parameters of the different fragility curves are listed in Table 1. It is evident that the shear failure is associated to lower PGA values, meaning that shear is the most probable failure mode considering both directions. This can be justified by the fact that most of the viaducts present in the database were built in the '70 s, when the code prescriptions on the shear reinforcement of piers were very poor. The high value of standard deviation indicates a great variation of the $PGA_C$ related to the shear failure, in contrast to the high slope of the curve, which is due to a low median value.

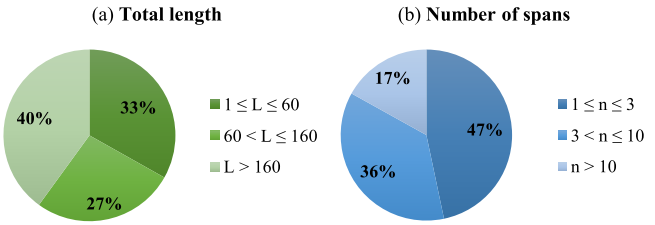


**Fig. 5.** – Classification of the bridges for (a) total length in m and (b) number of spans.

The sequence (from shear failure to unseating failure) and shape of the obtained curves are quite common, showing that the bending failure mode, associated to the exceeding of the ultimate bending moment at the base of the pier, usually is activated after the shear failure mode and way before the unseating one.

The different fragility curves reflect the different structural behavior of the structure along the two principal directions, depending on the geometry of the bridge. Generally, the behavior in the transverse direction is weaker, except in the case of unseating. This is related to the typical geometry of the pier cap that is generally characterized by a larger dimension in the transverse direction.

## 4. Granular fragility curves: bridge length and number of spans

With the aim to better understand the influence of certain characteristics of the bridge on the fragility curves, the considered bridge portfolio has been subdivided in sub-groups with respect to the total length (Fig. 5a) and the number of spans (Fig. 5b) of the bridges. The main information that comes out is that the majority of bridges have less than 3 spans (see also Fig. 1b). The bridges have been grouped in 3 categories to develop the macro-scale fragility curves:

- Short bridge: length between 1 m and 60 m (392) or number of spans between 1 and 3 (552);
- Medium bridge: length between 61 m and 160 m (317) or number of spans between 4 and 10 (430);
- Long bridge: length greater than 160 m (473) or number of spans greater than 10 (200).

The ranges of length and span were defined to guarantee an adequate number of bridges in all the groups, avoiding situations with few bridges in a group. Other grouping criteria of the structures can be considered, but this is out of the scope of the present work. In the following, the fragility curves for the different groups of bridges (short, medium, long) will be reported, according to the total length-based classification. The fragility curves obtained grouping the bridges on the basis of the number of spans are omitted because they show trends similar to the total length ones.

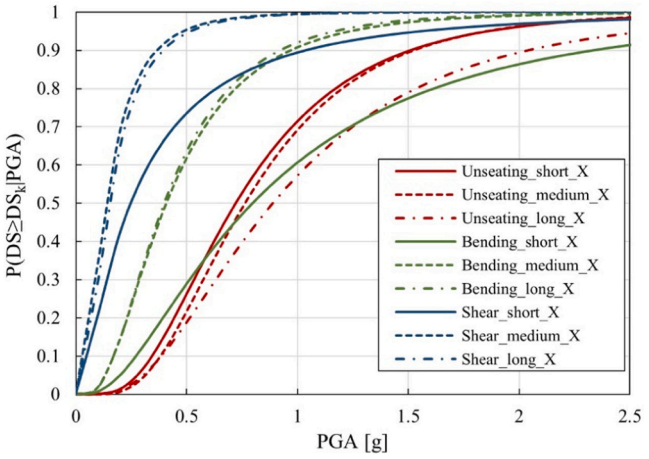


**Fig. 6.** – Fragility curves for total length grouping in longitudinal (X) direction.

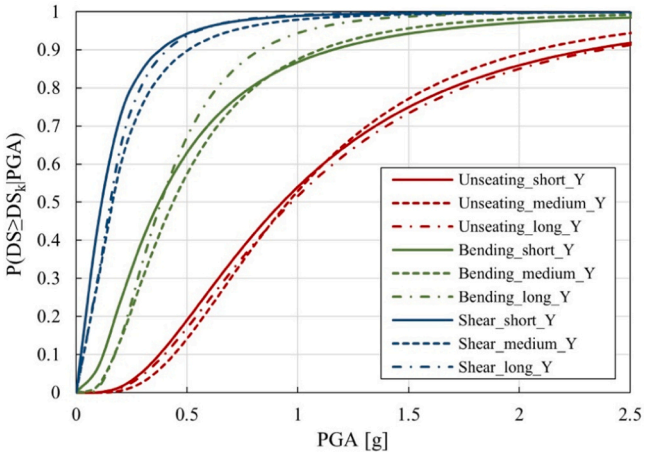


**Fig. 7.** – Fragility curves for total length grouping in transverse (Y) direction.

### 4.1. Bridge length-based fragility curves for the longitudinal direction

Fig. 6 shows the fragility curves of the considered highway bridges, grouped for the total length, in the longitudinal direction. The curves related to the short bridges (continuous lines) for the shear and bending failure modes are characterized by significantly higher mean PGA with respect to the corresponding cases of medium and long bridges. This difference is probably caused by the presence of a significant number of single-span bridges (112) in the short bridge group. For these kinds of bridges, only the unseating safety verifications could be performed because of the lack of piers in the structure. By removing the single-span bridges from the group of the short bridges, the trend of the short bridges fragility curves turns out to be similar to the corresponding one obtained considering the whole database of bridges.

The fragility curves related to the medium and long bridges, for both shear and bending failure, are very close to each other, while they are quite far in case of unseating failure. The higher vulnerability is associated to the shear failure.

### 4.2. Bridge length-based fragility curves for the transverse direction

Fig. 7 shows the fragility curves of the bridges, classified for the three ranges of the total length, in the transverse direction. The trend of the curves is similar to the one observed for the case of the whole stock. In this case, the differences among the three groups are less evident with respect to the case of the longitudinal direction. Particularly, the three curves related to the shear failure are very close or tend to overlap with each other. For the case of bending failure, the mean PGA is almost similar for the three groups of bridges, but the long bridges group is characterized by a lower logarithmic standard deviation, resulting in a different shape of the corresponding curve. The lowest median value is always related to the short bridges group, and the shear failure is the leading verification in the transverse direction.

## 5. Comparison with fragility curves from literature

The availability of modal pushover results for the described database allowed to evaluate the fragility curves of a large stock of Italian highway bridges and to make some considerations about their seismic vulnerability. Nevertheless, a comparison with similar results obtained on other stocks of bridges by other researchers could be useful to better understand the quality of the obtained results. Table 4 collects some references from other authors, which propose, for different RC bridge databases, the seismic vulnerability fragility curves obtained with different methodologies. The works are grouped with respect to the analysis method adopted to obtain the fragility curves. Some general characteristics about the bridges considered in each specific stock are also reported.

In the following sections, the comparison between the fragility curves obtained for the SIOS database and the literature ones is presented, considering the adopted different analysis methods.

### 5.1. Vulnerability analyses with NLTHA method

The first group of considered research papers adopts the non-linear time history analysis (NLTHA) for the assessment of the structures. The main characteristics of the stock of bridges analyzed in each work are briefly recalled in the following.

Choi et al. [20] studied a stock of bridges located in the central and southeastern United States, with different structural schemes. The 95 %

**Table 4 –**
Available studies on fragility curves of bridges.

| Research paper | Site | Analysis type | Seismic input | Bridge typology | Number of spans | Number of bridges* |
|---|---|---|---|---|---|---|
| Choi et al. (2004) [20] | USA | NLTHA | Accelerograms (100) | MSC+MSSS | 3 | 20 |
| Nielson et al. (2007) [21] | USA | NLTHA | Accelerograms (96) | MSC+MSSS+SS | 3 | 78319 |
| Banerjee et al. (2008) [22] | California | NLTHA | Accelerograms (60) | MSC | 5, 10, 12 | 3 |
| Jeon et al. (2015) [23] | California | NLTHA | Accelerograms (114) | MSC | 2 | 1 |
| Zhang et al. (2009) [24] | Mendocino, California | NLTHA | Accelerograms (250) | MSC | 4 | 1 |
| Alipour et al. (2011) [25] | Los Angeles, California | NLTHA | Accelerograms (60) | MSC | 2, 3 | 6 |
| Avşar et al. (2011) [26] | Turkey | NLTHA | Accelerograms (25) | MSC | $\geq 2$ | 52 |
| Borzi et al. (2015) [27] | Italy | IRHA | Response spectrum | MSC+MSSS | $\leq 5$ | 9 |
| Moschonas et al. (2009) [28] | Greece | NLSA | Response spectrum | MSC | $2 \div 12$ | 62 |
| Perdomo et al. (2022) [29] | Italy | NLSA | Response spectrum | MSC | 8, 9, 13, 31 | 4 |
| Cardone et al. (2011) [30] | Campania, Italy | IACSM | Response spectrum | MSSS | $\geq 2$ | 5 |
| Miano et al. (2016) [31] | Campania, Italy | IACSM | Response spectrum | MSSS | $\geq 2$ | 5 |

*The number refers only to the bridges considered for the comparison.

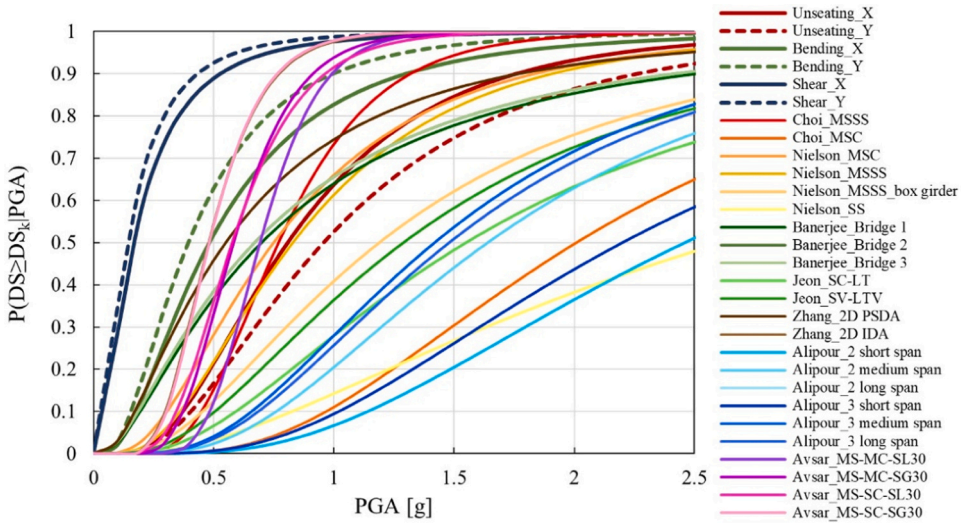


**Fig. 8.** – Comparison between the fragility curves of the SIOS stock and the ones from NLTHA literature.

of the database is represented by multi-span continuous (MSC) bridges, multi-span simply supported (MSSS) bridges, and single span (SS) bridges. For the comparison with the SIOS stock of highway bridges, only MSC and MSSS bridges will be considered. Nonlinear finite element models were created to generate the fragility curves by using about one hundred accelerograms. Four different damage levels were analyzed using the software HAZUS 97. The fragility curves were developed first for the bridge structural components and later combined to obtain the global fragility curves. For the comparison, only the fragility curves obtained for the extensive damage will be considered.

Nielson et al. [21] also considered a database of bridges located in the central and southeastern United States. More than 100000 bridges, classified in nine different classes, were analyzed. The classes that will be considered for the comparison are: MSSS bridges with concrete girder, MSSS bridges with concrete box girder, MSC bridges, and SS bridges. Three-dimensional numerical models were developed and analyzed through non-linear dynamic analysis by using about one hundred accelerograms. The fragility curves were obtained establishing a relationship between the PGA and the probability of exceedance for four different damage states, according to the definition given by the FEMA-356 [3]. For the comparison, only the fragility curves for extensive damage will be considered.

Banerjee et al. [22] developed analytical fragility curves for three representative RC bridges with the following characteristics: (i) 5 spans bridge with 4 round section piers, one expansion joint, and a 3-cell concrete box girder deck, (ii) 12 spans bridge with 11 oblong columns, one expansion joint, and a 4-cell concrete box girder deck, (iii) 10 spans bridge with 9 rectangular section columns of different heights, 4 expansion joints, and a 5-cell concrete box girder deck. 2D nonlinear analyses were performed using 60 earthquake time histories developed for a FEMA/SAC project, subdivided into 3 groups with different exceeding probabilities. The structural response was measured in terms of rotational ductility and shear force at column ends. Four different damage states were considered as defined by HAZUS 99 [49], but only the extensive damage state will be considered for the comparison.

Jeon et al. [23] proposed the study of a two span single frame concrete box girder highway bridge built in California in 1967. The spans show different lengths, with a 6 m high pier. The research was focused on the study of the shear behavior of the pier. Four different models were developed for the same geometry by changing the input ground motions (e.g., longitudinal, transverse or vertical) and the pier behavior model (e.g., bending, bending+shear). Only two models will be considered for the comparison: a pier shear model under constant axial load (gravity load) with longitudinal and transverse ground motions (named SC-LT), and a pier shear model under multiple levels of axial load with ground motions in all the three orthogonal directions (named SC-LTV). A total of 114 ground motions were used for the non-linear time history analyses, measuring the demand in terms of maximum pier drift (in percentage). The damage states to develop the fragility curves were defined according to previous study. For the comparison with the fragility curves of the SIOS database, only the extensive damage state will be considered.

Zhang et al. [24] selected a typical highway bridge, built in California before 1971, to derive the fragility curves. The structure is a four-span continuous concrete box girder bridge with monolithic abutments and piers having different heights (from 7.6 m to 9.6 m). The bridge was studied in the as-built configuration and in the retrofitted configuration, using different seismic isolation devices, developing both 2D and 3D finite element models. For the comparison, only the results obtained from the simplified 2D model of the as-built configuration (i.e., without isolation devices) will be considered. The fragility curves were derived using the Probabilistic Seismic Demand Analysis (PSDA) and the Incremental Dynamic Analysis (IDA). The PSDA uses unscaled earthquake ground motions to obtain a correlation between the engineering demand parameters (i.e., section curvature of the pier) and the ground motion intensity measures (PGA). In the IDA approach, all the accelerograms are scaled to selected intensity levels associated to prescribed seismic hazard levels, and the non-linear time history analyses are performed for each different hazard level. For comparison, only the fragility curves obtained from the simplified 2D model for the extensive damage state will be considered.

Alipour et al. [25] studied the life-cycle performance and cost of RC highway bridges subjected to earthquake ground motions while they are continuously exposed to corrosion. Several bridge models with different structural characteristics were developed to evaluate the influence of the corrosion process on the structural capacity and seismic performance of bridges. The fragility curves were developed for different ages of the bridges, by properly updating the properties of RC members at each stage. 18 box girder bridges with two or three spans, different column properties (height and cross-section), and various span lengths (short, medium or long) were modeled. For a fair comparison, only the curves related to undamaged bridges will be extracted, considering bridges with two and three spans, with 10 m high piers (medium height), and all the span length options. A set of 60 earthquake ground motions was considered to generate the fragility curves, and the pier curvature ductility (i.e., the ratio between the maximum pier curvature recorded from the nonlinear time-history analysis and the pier yield curvature obtained from moment-curvature analysis) is assumed as the damage intensity measure. For the comparison, only the fragility curves related

**Table 5 –**
NLTHA fragility curves parameters.

| Reference | Structure | $x_m$ [g] | β |
|---|---|---|---|
| Choi et al. [20] | MSSS | 0.770 | 0.420 |
| Choi et al. [20] | MSC | 2.010 | 0.570 |
| Nielson et al. [21] | MSC | 0.750 | 0.700 |
| Nielson et al. [21] | MSSS | 0.830 | 0.650 |
| Nielson et al. [21] | MSSS concrete box girder | 1.190 | 0.750 |
| Nielson et al. [21] | SS | 2.620 | 0.900 |
| Banerjee et al. [22] | Bridge 1 | 0.700 | 1.000 |
| Banerjee et al. [22] | Bridge 2 | 0.670 | 1.000 |
| Banerjee et al. [22] | Bridge 3 | 0.670 | 1.000 |
| Jeon et al. [23] | SC-LT | 1.550 | 0.750 |
| Jeon et al. [23] | SV-LTV | 1.290 | 0.730 |
| Zhang et al. [24] | 2D model PSDA | 0.550 | 0.910 |
| Zhang et al. [24] | 2D model IDA | 0.480 | 0.370 |
| Alipour et al. [25] | Short span, 2 spans | 2.460 | 0.600 |
| Alipour et al. [25] | Medium span, 2 spans | 1.640 | 0.600 |
| Alipour et al. [25] | Long span, 2 spans | 1.480 | 0.600 |
| Alipour et al. [25] | Short span, 3 spans | 2.200 | 0.600 |
| Alipour et al. [25] | Medium span, 3 spans | 1.420 | 0.600 |
| Alipour et al. [25] | Long span, 3 spans | 1.480 | 0.600 |
| Avsar et al. [26] | MS-MC-SL30 | 0.693 | 0.280 |
| Avsar et al. [26] | MS-MC-SG30 | 0.583 | 0.350 |
| Avsar et al. [26] | MS-SC-SL30 | 0.577 | 0.400 |
| Avsar et al. [26] | MS-SC-SG30 | 0.482 | 0.360 |

to the extensive damage state will be considered.

Avşar et al. [26] developed analytical fragility curves for a group of 52 RC highway bridges built after the 1990s in Turkey. The inventory includes multi-span (MSSS) composite structures with prestressed concrete girders and continuous cast-in-place RC decks. The bridges were grouped into 4 main classes, supposing a similar seismic behavior for the bridges of the same class. The classification was based on the available data from past earthquake reports and previous studies to define the bridges primary structural attributes (i.e., number of spans, number of piers, and skew angle). Comprehensive 3D finite element models of the bridges were subjected to nonlinear time history analyses. A set of 25 accelerograms recorded in Turkey and in other regions having similar faulting mechanisms and seismic potential were used to generate the fragility curves. The curvature of the pier and of the cap beam was assumed as the damage intensity measure, as well as the shear in the pier and the displacement of the deck. The lognormal distribution fragility curves were developed for several seismic intensity measures (i.e., PGA, peak ground velocity, acceleration spectrum intensity). The fragility curves considered for the comparison with the ones of the SIOS database are those having the PGA as IM and referred to the extensive damage state.

### 5.2. Comparative graph and remarks about NLTHA fragility curves

Fig. 8 shows the comparison between the 23 fragility curves extracted from the presented references which adopted the NLTHA method and the six fragility curves of the whole stock of bridges of the SIOS database. The main parameters of each fragility curve are listed in Table 5.

It could be observed that the shape of the fragility curves and their respective main parameters are influenced by several aspects.

The first element to be considered is the size of the bridge inventory. The fragility curves that consider only a single typical bridge ([20,21]) show lower coefficients of variation with respect to other curves which refer to bigger inventories (e.g., [23] which considers 78319 bridges). Moreover, sometimes, it is difficult to consider them as representative of an entire bridge category. The strong point of the SIOS fragility curves with respect to the other ones is that they are obtained using a huge inventory of existing bridges, individually analyzed (only reference [21] has a bigger stock).

The structural typology of the bridge is another crucial element. Most of the studies deal with MSC bridges and only some of them also consider MSSS bridges. In the work presented by Choi et al. [20], the results for these two typologies can be compared, highlighting that the MSC typology turns out to be the less vulnerable, thanks to the continuity of the deck structure. A different conclusion can be made by observing the fragility curves proposed by Nielson et al. [21]. In particular, the fragility curves related to MSSS and MSC concrete box girder bridges are very close between them and with the SIOS database curves associated to the unseating failure. It is also interesting to notice that the fragility curve proposed in [21] and related to SS bridge shows a lower vulnerability. In this configuration, where the deck is supported only by the abutments, it should be expected that the [21] SS bridge fragility curve will be close to the fragility curve associated to the unseating failure of SIOS database. Instead, this is not the case, probably because the SS bridges represent only the 9 % of the bridge analyzed stock, and also because the coefficient of variation obtained by Nielson et al. [21] is quite higher than the one reported in Section 3.2 (0.9 vs 0.607).

The fragility curves for two or three spans' bridges proposed by Alipour et al. result to be shifted to the right with respect to the six curves of the SIOS database. This could be due to the limited dimensions of the structures and to the reduced number of piers, following in a better seismic performance.

The methodology to derive the analytical fragility function may also influence the resulting fragility curves as proved by the work of Zhang et al. [24]. Indeed, the curve related to the IDA method is associated to a more conservative configuration (with lower coefficient of variation) with respect to the one obtained with the PSDA method. Moreover, both these two curves fall within the range of the fragility curves determined in this work.

Generally, the fragility curves obtained for the SIOS bridge stock are close to the others available in the literature, with the ones related to the shear and bending failure modes placed on the left side of the bundle of curves taken from the literature references. It is important to underline that the fragility curves available in literature do not distinguish between the different failure modes, showing only the most restrictive one.

To better understand the differences between the proposed fragility curves and those reported in the literature, it should be noted that the fragility curves of the SIOS database are obtained by modal pushover analysis following the procedure described in ATC-40. Therefore, the mean value of the failure PGA is somewhat on the safe side due to the overestimation of the equivalent damping coefficient implied by the use of the ATC-40 method in the pushover analysis [50]. Another source of difference between the proposed fragility curves and those in the literature is related to the lack of record-to-record variability implied by the use of NLSA with smoothed spectrum, which results in an underestimation of the lognormal standard deviation. However, the underestimation of the standard deviation related to the lack of record-to-record variability is partially compensated by the large variability of the real configurations considered related to the high sample size in the database.

Overall, the results show the effectiveness of the nonlinear static analysis (NLSA) which allows to obtain reliable results with lower computational effort with respect to the NLTHA, staying on the safe side.

### 5.3. Vulnerability analyses with IRHA method

The Inelastic Response History Analysis (IRHA) method was adopted by Borzi et al. [27] to evaluate specific fragility curves on an Italian bridge stock, within the framework of a Civil Protection sponsored project. The database included 485 bridges, whose most common characteristics were: less than five spans, single piers with height ranging between 10 m and 20 m, box girder cross section, and simply supported decks with elastomeric bearings. The aim of the work was to map the bridge seismic risk at national level, giving real-time damage-probability scenario.

The fragility curves were evaluated by Borzi et al. [27] for nine

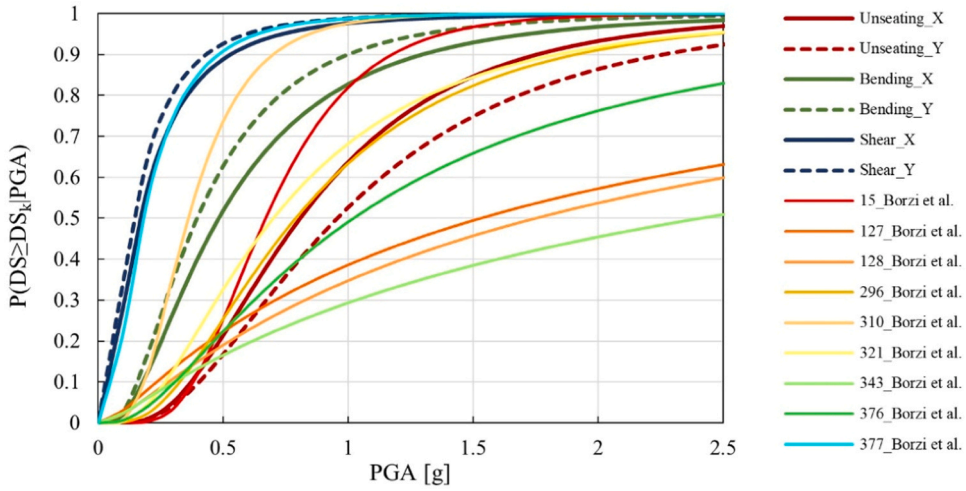


**Fig. 9.** – Comparison between the fragility curves of the SIOS stock and the ones from Borzi et al. [27].

**Table 6 –**
Parameters of the fragility curves by Borzi et al. [27].

| Bridge ID | $x_m$ [g] | β |
|---|---|---|
| 15 | 0.670 | 0.440 |
| 127 | 1.530 | 1.470 |
| 128 | 1.750 | 1.430 |
| 296 | 0.790 | 0.690 |
| 310 | 0.360 | 0.520 |
| 321 | 0.700 | 0.750 |
| 343 | 2.410 | 1.620 |
| 376 | 1.020 | 0.940 |
| 377 | 0.180 | 0.770 |

**Table 7 –**
NLSA fragility curves parameters.

| Reference | Bridge ID | $x_m$ [g] | β |
|---|---|---|---|
| Moschonas et al. [28] | 122Y | 0.281 | 0.650 |
| Moschonas et al. [28] | 232Y | 0.686 | 0.650 |
| Moschonas et al. [28] | 332Y | 0.983 | 0.600 |
| Perdomo et al. [29] | 13 | 1.515 | 0.400 |
| Perdomo et al. [29] | 14 | 0.824 | 0.400 |
| Perdomo et al. [29] | 17 | 0.286 | 0.600 |
| Perdomo et al. [29] | 28 | 0.529 | 0.300 |

increasing values of PGA, with a mean return period of exceedance ($T_R$) ranging from 30 to 2475 years, as required by the Italian Standard [4]. For each intensity level, a number of artificial spectrum-compatible ground motions were generated, and, for these motions, the IRHA provided the demand values D on each bridge component. These values were then compared to the corresponding capacity values C of each element, depending on the considered damage state. The demand-to-capacity ratio Y=D/C was then used to measure the global structural performance. Furthermore, the values of Y calculated for each damage state were then used to develop a lognormal distribution in order to estimate the exceeding probability of the unit value of Y, associated to the failure onset.

A total of 180 IRHA analyses were performed for each bridge (ten artificial motions, for nine PGA values, for two different modeling assumptions on the bearings). For the comparison with the SIOS bridge stock, only the fragility curves related to the damage state closest to the extensive damage state were considered. Although the definition of damage states is slightly different for the two stocks of bridges, the comparison seemed interesting because the two databases belong to the same infrastructural system (i.e., Italian RC highway viaducts). Finally, within the stock of 485 bridges, nine bridges were selected as representative of the most common typology (simply supported multi-span decks, single-stem hollow section piers, piers height between 5 m and 30 m, and rubber bearings), and the corresponding fragility curves reported in [27].

#### 5.3.1. *Comparative graph and remarks about IRHA fragility curves*

Fig. 9 shows the comparison between the fragility curves obtained for the whole SIOS stock and the ones provided by Borzi et al. [27] following the IRHA approach. The main parameters of each fragility curve are listed in Table 6.

Before discussing the comparison between the fragility curves, it should be underlined that their shapes are strongly affected by several characteristics of the analyzed bridges or the homogeneity of the group of considered structures. In fact, Fig. 9 clearly shows that, even if the nine selected bridges analyzed in [27] are quite similar, their fragility curves are very different. It is also evident that the shear failure fragility curves (in both longitudinal and transverse directions) of the whole SIOS database are almost coincident with the one of bridge 377 and very close to the one related to the bridge 310, which corresponds to the longest bridges (448 m and 425 m, respectively) with the highest number of spans (13 and 12, respectively). This could be explained because, as presented in Section 2, the whole SIOS database mainly collects long bridges. Fragility curves of bridges 15, 321, and 376, which show an "intermediate" number of spans and lengths (7, 6, and 9 spans; and 236 m, 211 m, and 305 m, respectively), come right after. The other curves (bridges 127, 128, 296, and 343) are more similar to the fragility curves of the whole SIOS database related to the unseating failure, probably because these bridges are the ones with the lower length and span number, showing a higher seismic resistance (i.e., high median values) together with a high dispersion of the results (i.e., high standard deviation).

Generally, it is evident that the results of the most critical failure mode (first shear failure of a pier) related to the whole stock of SIOS bridges are located on the left side of the plot, confirming the conservative approach of the pushover analyses with respect to the dynamic ones (like the IRHA method).

### 5.4. *Vulnerability analyses with NLSA method*

The group of research papers considered in this section adopts the nonlinear static analysis (NLSA), i.e. the same approach adopted to develop the fragility curves of the SIOS database.

Moschonas et al. [28] developed the fragility curves for the most common Greek highway bridge typologies. In particular, the research

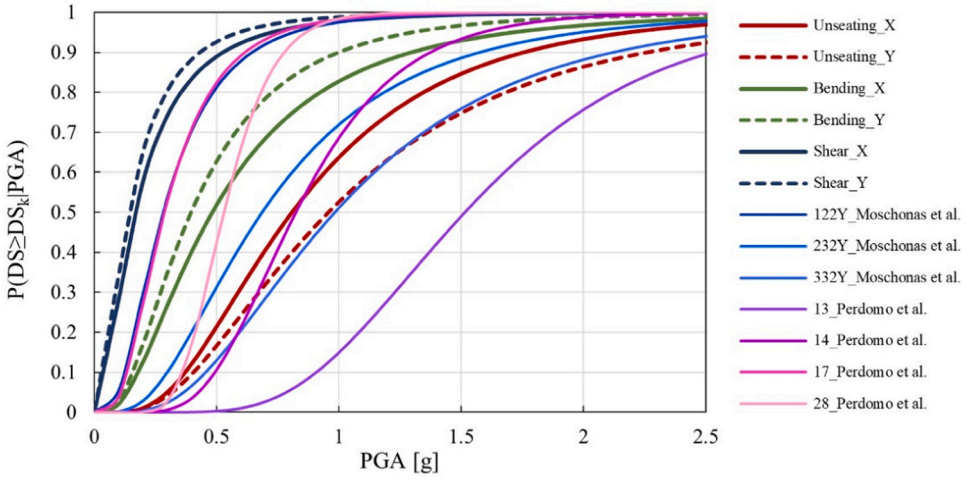


**Fig. 10.** – Comparison between the fragility curves of the SIOS stock and the ones from NLSA literature.

was focused on the bridges located on the Egnatia Odos highway, in the northern part of Greece. The bridges were grouped according to the main characteristics affecting the seismic behavior: type of pier, type of deck, and type of piers-to-deck connection, obtaining a total of 11 groups. The methodology proposed by Moschonas et al. is based on the pushover analysis of the bridges, according to the capacity spectrum method, and is similar to the one adopted in HAZUS [49]. The bridges were classified into two main categories according to their seismic energy dissipation mechanism: (i) column/framed pier bridges, with yielding piers, and (ii) wall type pier bridges, with elastic piers and nonlinear bearing devices. The damage states were defined according to Basöz et al. [51], using damage parameters. For the comparison with the SIOS database results, only the fragility curves related to the extensive damage state were considered. The demand parameter is measured through the maximum displacement of the bridge, according to the nonlinear behavior of piers/bearings, as a function of the PGA.

Perdomo et al. [29] studied the accuracy and suitability of NLSA procedures for the development of analytical fragility curves for seismic risk assessment of large portfolios of RC bridges with single or multiple piers. Several approaches were used to develop the curves (e.g., modal pushover analysis, capacity spectrum method, etc.), but only the results obtained from the modal pushover analysis were considered in the following for comparison with SIOS database curves, for the sake of homogeneity. The portfolio includes 50 RC Italian bridges with single-stem piers, grouped in “classical” (C) and “non-classical” (NC) bridges, based on the participating mass of the first vibration mode. The C bridges show a dominant first (fundamental) vibration mode, in which all piers move in the same direction, while the NC bridges are always higher-mode sensitive. The damage states were defined according to the criteria proposed by HAZUS [49] and the pier displacement ductility was adopted as demand parameter. For the comparison with the SIOS fragility curves, only 4 configurations over 50 were considered, 2 belonging to the C bridges (i.e., bridges 4 and 17) and 2 belonging to the NC bridges (i.e., bridges 13 and 28), limiting the comparison to the extensive damage state. The IM is assumed as the spectral acceleration at the fundamental period $S_a(T_1)$, which is different from the IM adopted in the other discussed works (i.e., the PGA). For this reason, a conversion was made to make possible the comparison of the curves. Given that all the analyzed bridges were in Italy, the Italian lithostatic map based on the soil type classes of the EC8 [32] elastic response spectrum was used for the $S_a(T_1)$-PGA conversion.

#### 5.4.1. *Comparative graph and remarks about NLSA fragility curves*

The comparison between the fragility curves of the SIOS portfolio and the ones obtained by other authors with the NLSA approach (Fig. 10) considers only the behavior in the transverse direction of the bridge, according to the literature available data. The SIOS curves fit well inside the bundle of the other fragility curves, proving the reliability of the proposed approach. The fragility curve related to the shear still remains the most vulnerable one, followed by the curve associated with the bridge 122Y (4 spans, simply-supported box girder deck, 180 m, single-stem pier with circular section) and bridge 17 (same column type and similar length of 122Y). The bridge 232Y is less vulnerable than the previous two, even though it is also a simply-supported bridge with single column. Bridge 28 is the longest one (852.5 m with 31 spans) and for this reason its fragility curve is located among the most vulnerable ones, even if its high steep is associated with a very low standard deviation, which makes the curve cross the SIOS curve related to the bending failure. It is interesting to notice the similarity between the curve of bridge 332Y and the SIOS fragility curve related to the unseating failure, which is probably due to the fact that the majority of the bridges of the SIOS portfolio have 3 spans as bridge 332Y.

As a final comment, it should be emphasized that the SIOS portfolio fragility curves are related to a large stock of bridges (thus including very different bridge geometries), whereas the curves proposed in the literature for NLSA are single bridge fragility curves. This makes the comparison difficult as the logarithmic standard deviation is very different due to the large difference in the variability of the bridge geometry. Nevertheless, the SIOS database fragility curves are on the safe side with respect to those proposed in the literature.

### 5.5. *Performance-based adaptive analyses with IACSM-DAP method*

The main aim of the Inverse Adaptive Capacity Spectrum Method (IACSM) is the evaluation of the earthquake intensity level (e.g., PGA) corresponding to pre-established damage states of the structure, identified by given performance points on the capacity curve of the bridge. Consequently, since the inelastic deformed shape of the bridge related to each damage state is known from the beginning of the analysis, the equivalent damping ratio of the bridge can be directly estimated by properly combining the damping contributions of each member of the bridge. Contrary to the direct approach, IACSM is not iterative and does not require the bilinearization of the capacity curve of the equivalent single degree of freedom (SDOF) model of the bridge.

Instead of using the conventional force-based methods, the capacity curves of the bridge may be evaluated with the Displacement Adaptive Pushover (DAP) analysis to better estimate the deformed shape and the distribution of the internal actions in the structural elements. The seismic vulnerability is then evaluated for a number of Performance

**Table 8 –**
IACSM-DAP fragility curves parameters.

| Reference | Bridge ID | $x_m$ [g] | β |
|---|---|---|---|
| Cardone et al. [30] & Miano et al. [31] | Lauretta | 0.500 | 0.570 |
| Cardone et al. [30] & Miano et al. [31] | Ceraso | 0.420 | 0.600 |
| Cardone et al. [30] & Miano et al. [31] | Castello | 0.820 | 0.640 |
| Cardone et al. [30] & Miano et al. [31] | San Gennaro | 0.700 | 0.610 |
| Cardone et al. [30] & Miano et al. [31] | Carapelle | 0.680 | 0.610 |

Levels (PL), each one associated with a number of damage states of the critical members of the bridge, identified by a series of points on the DAP curve.

Cardone et al. introduced the IACSM-DAP approach in [30] to determine the fragility curves (and the risk index) of an Italian highway bridge portfolio. The different PLs associated to the different DSs were first defined. From the finite element model, the capacity curves of the equivalent SDOF models were determined. Lastly, after the evaluation of the equivalent viscous damping, the seismic demand (PGA) associated to each damage state was determined and used to derive the lognormal fragility curves, which gives the exceedance probability of the considered damage state as a function of the PGA of the expected ground motion.

A set of 9 bridges located on the Italian A16 highway were analyzed, considering the most representative configurations (multi-span bridges, with simply supported decks and mean span of 33 m). All the bridges were built between 1969 and 1971 without seismic provisions and in moderate/high seismicity regions. For this reason, the results show a high vulnerability for these structures. Subsequently, Miano et al. [31] presented other similar evaluations for the same bridge portfolio, used to extrapolate the fragility curve main parameters reported in the following (Table 8).

*5.5.1. Comparative graph and remarks about IACSM-DAP fragility curves*

Fig. 11 shows the comparison between the SIOS database fragility curves and the ones obtained with the IACSM-DAP approach, particularly for the five bridges Lauretta, Cesaro, Castello, San Gennaro, and Carapelle. It is remarkable the similarity of these fragility curves, with the five bridges falling within the bundle of SIOS database. It should be noticed that the SIOS portfolio collects a huge number of bridges, while the IACSM-DAP considers only five bridges, so the comparison may not be equilibrated. The most vulnerable structures are Ceraso and Lauretta, whose main common characteristics are the pier type (i.e., single-stem pier) and the number of spans (5). These curves intersect the SIOS curve of the bending failure, probably because they have a similar PGA mean value with a low standard deviation. Carapelle and San Gennaro bridges show similar curves; the first one has 5 spans while the second 3, and both of them are supported by wall piers. This type of pier often shows a higher resistance with respect to the single-stem pier, turning out to a less fragility for this kind of bridges. The less vulnerable curve is the one of the Castello bridge, which have only 2 spans and a single wall pier. The curve results quite similar to the SIOS curve associated to the unseating failure, being the 2 spans structure less sensible to flexural and shear failures.

## 6. Conclusions

The aim of this study was to evaluate the seismic vulnerability of a portfolio (1182 bridges) of Italian highway RC viaducts. All the available data (pictures, original drawings, and documents) have been used to accurately model each bridge of the considered portfolio, implementing detailed 3D finite element models to be used in the structural analyses for the shear, bending and unseating limit state verifications. This is a strong point compared to other studies available in scientific literature, which are usually based on a smaller number of structures or parametric geometries of the bridges.

For each modelled bridge, nonlinear static analyses were performed. Considering the number of bridges to be analyzed (more than one thousand), this method allowed to save a lot of computational time with respect to the more accurate nonlinear dynamic approach. An ad-hoc developed software (MPA_CISE) was used to perform the modal pushover analyses, determining the performance point and the corresponding failure PGA against all the considered failure modes, for each modelled bridge. The PGA was used as intensity measure of the seismic action, which was then associated to the probability of exceeding of the extensive damage limit state. The obtained results were used to generate the fragility curves in the two main directions of the bridges (longitudinal and transverse), for the three considered failure modes, using another specifically developed software (FC_Gen). Therefore, the obtained fragility curves are referred not to individual bridges but to a bridge class that accounts for the different bridge geometries, structural types, and material properties. Due to the assumption of a smoothed response spectrum in the modal pushover analyses, the record-to-record variability was not considered.

The fragility curves showed that shear failure of the pier is the first failure mechanism activated, followed by the bending failure of the pier, and, with significantly higher values of PGA, by the unseating of the deck.

The whole SIOS database of bridges was then divided into subgroups based on the total length of the bridge and the number of spans. For each subgroup of bridges, the fragility curves were determined and, also in

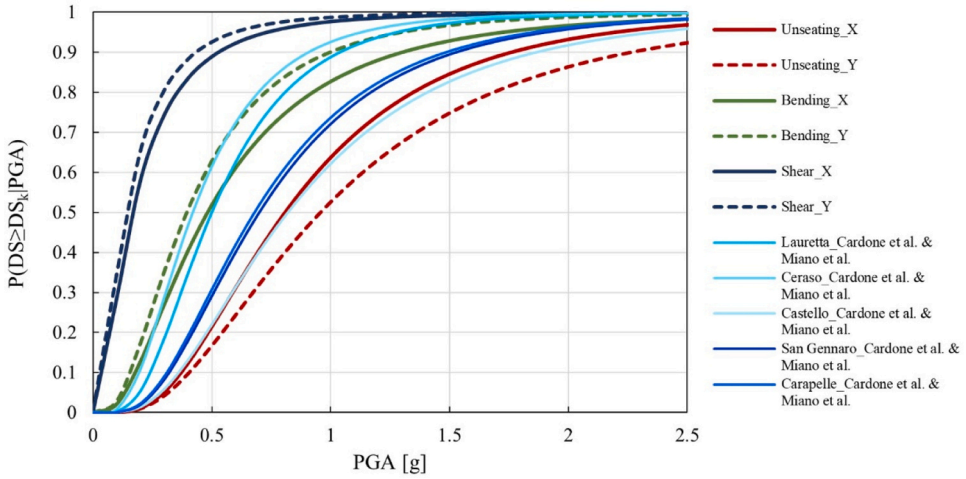


**Fig. 11.** – Comparison between the fragility curves of the SIOS stock and the ones from IACSM-DAP literature.

this case, it was found that, for low values of PGA, the probability of collapse for shear failure of the pier is quite high. Moreover, looking at the median values of the fragility curves for shear failure, it comes out that, in the longitudinal direction, the "short" bridges are the least vulnerable while the "medium" ones are the most vulnerable. In the transverse direction, the short bridges are characterized by the lowest median value of PGA.

In order to validate the adopted approach and the obtained results, a comparison was made with fragility curves collected from the scientific literature. Several studies on bridges with similar characteristics were considered and classified on the basis of the analysis method adopted to obtain the fragility curves. The comparison showed that the SIOS fragility curves were close to those available in the literature and sometimes placed within the bundle of fragility curves reported by other researchers. Nevertheless, it should be highlighted that, in some cases, the differences between the hypotheses made in the considered approaches made the comparison not always simple.

The obtained fragility curves could be implemented by the highway authority in the bridge management software to evaluate possible intervention scenarios and schedule the proper maintenance retrofitting works to improve the infrastructural network performance.

Future developments of the research could include different groupings of the bridges and the study of the influence of corrosion and maintenance interventions on the fragility curves.

## CRediT authorship contribution statement

**Rocco Buoninconti:** Visualization, Validation, Investigation, Formal analysis, Data curation. **Pietro Crespi:** Writing – review & editing, Writing – original draft, Validation, Supervision, Project administration, Methodology, Investigation, Formal analysis, Conceptualization. **Manuela Scamardo:** Writing – review & editing, Writing – original draft, Visualization, Methodology, Investigation, Formal analysis, Data curation.

## Declaration of Competing Interest

The authors declare that they have no known competing financial interests or personal relationships that could have appeared to influence the work reported in this paper.

## Acknowledgments

The authors would like to thank Dr. Nicola Giordano for his fundamental contribution in the successful completion of this study. Many thanks also to Eng. Giuseppe Pasqualato and Eng. Alberto Contardi, from SINA Engineering company, who provided the bridges database used for this research.

## References

[1] Simon J, Bracci JM, Gardoni P. Seismic response and fragility of deteriorated reinforced concrete bridges. J Struct Eng 2010;136:1273–81. https://doi.org/10.1061/(ASCE)ST.1943-541X.0000220.
[2] De Risi R, Di Sarno L, Paolacci F. Probabilistic seismic performance assessment of an existing RC bridge with portal-frame piers designed for gravity loads only. Eng Struct 2017;145:348–67. https://doi.org/10.1016/J.ENGSTRUCT.2017.04.053.
[3] FEMA 356. FEMA 356 - Prestandard and commentary for the seismic rehabilitation of buildings, FEDERAL EMERGENCY MANAGEMENT AGENCY. 2000.
[4] NTC2018 IM of I. Norme Tecniche per le Costruzioni. DM 17/1/2018 (in Italian). Gazzetta Ufficiale Della Repubblica Italiana 2018.
[5] Zucca M, Crespi P, Stochino F, Puppio ML, Coni M. Maintenance interventions period of existing RC motorway viaducts located in moderate/high seismicity zones. Structures 2023;47:976–90. https://doi.org/10.1016/j.istruc.2022.11.135.
[6] Ventura R, Maternini G, Barabino B. Traffic hazards on main road's bridges: real-time estimating and managing the overload risk. IEEE Trans Intell Transp Syst 2024:1–17. https://doi.org/10.1109/TITS.2024.3371265.
[7] Lipari A, Caprani CC, OBrien EJ. A methodology for calculating congested traffic characteristic loading on long-span bridges using site-specific data. Comput Struct 2017;190:1–12. https://doi.org/10.1016/j.compstruc.2017.04.019.
[8] Chen Z, Bao Y, Chen J, Li H. Modelling the spatial distribution of heavy vehicle loads on long-span bridges based on undirected graphical model. Struct Infrastruct Eng 2019;15:1485–99. https://doi.org/10.1080/15732479.2019.1639774.
[9] Enright B. O'Brien EJ. Monte Carlo simulation of extreme traffic loading on short and medium span bridges. Struct Infrastruct Eng 2013;9:1267–82. https://doi.org/10.1080/15732479.2012.688753.
[10] Khan SU, Ayub T, Qadir A. Effect of overloaded vehicles on the performance of highway bridge girder: a case study. Procedia Eng 2014;77:95–105. https://doi.org/10.1016/j.proeng.2014.07.010.
[11] Zucca M, Reccia E, Longarini N, Eremeyev V, Crespi P. On the structural behaviour of existing RC bridges subjected to corrosion effects: numerical insight. Eng Fail Anal 2023;152. https://doi.org/10.1016/j.engfailanal.2023.107500.
[12] Berto L, Vitaliani R, Saetta A, Simioni P. Seismic assessment of existing RC structures affected by degradation phenomena. Struct Saf 2009;31:284–97. https://doi.org/10.1016/J.STRUSAFE.2008.09.006.
[13] Zhang G, Liu Y, Liu J, Lan S, Yang J. Causes and statistical characteristics of bridge failures: a review. J Traffic Transp Eng (Engl Ed 2022;9:388–406. https://doi.org/10.1016/j.jtte.2021.12.003.
[14] Chen L, Wu H, Liu T. Vehicle collision with bridge piers: a state-of-the-art review. Adv Struct Eng 2021;24:385–400. https://doi.org/10.1177/1369433220953510.
[15] OPCM 3274. Primi elementi in materia di criteri generali per la classificazione sismica del territorio nazionale e di normative tecniche per le costruzioni in zona sismica (in Italian). Gazzetta Ufficiale Della Repubblica Italiana, GU 2003;105.
[16] DPC/SISM/0092847. Archiviazione e trasmissione dei dati delle schede di livello 0, 1 e 2 delle verifiche sismiche di opere strategiche e rilevanti (in Italian). Circolare Dipartimento Protezione Civile 2010.
[17] Frangopol DM, Liu M. Maintenance and management of civil infrastructure based on condition, safety, optimization, and life-cycle cost*. Struct Infrastruct Eng 2007;3:29–41. https://doi.org/10.1080/15732470500253164.
[18] Monteiro R, Zelaschi C, Silva A, Pinho R. Derivation of fragility functions for seismic assessment of RC bridge portfolios using different intensity measures. J Earthq Eng 2019;23. https://doi.org/10.1080/13632469.2017.1387188.
[19] Abarca A, Monteiro R, O'Reilly G, Zuccolo E, Borzi B. Evaluation of intensity measure performance in regional seismic risk assessment of reinforced concrete bridge inventories. Struct Infrastruct Eng 2023;19. https://doi.org/10.1080/15732479.2021.1979599.
[20] Choi E, DesRoches R, Nielson B. Seismic fragility of typical bridges in moderate seismic zones. Eng Struct 2004;26. https://doi.org/10.1016/j.engstruct.2003.09.006.
[21] Nielson BG, DesRoches R. Analytical seismic fragility curves for typical bridges in the central and southeastern United States. Earthq Spectra 2007;23. https://doi.org/10.1193/1.2756815.
[22] Banerjee S, Shinozuka M. Mechanistic quantification of RC bridge damage states under earthquake through fragility analysis. Probabilistic Eng Mech 2008;23. https://doi.org/10.1016/j.probengmech.2007.08.001.
[23] Jeon JS, Shafieezadeh A, Lee DH, Choi E, DesRoches R. Damage assessment of older highway bridges subjected to three-dimensional ground motions: characterization of shear-axial force interaction on seismic fragilities. Eng Struct 2015;87. https://doi.org/10.1016/j.engstruct.2015.01.015.
[24] Zhang J, Huo Y. Evaluating effectiveness and optimum design of isolation devices for highway bridges using the fragility function method. Eng Struct 2009;31. https://doi.org/10.1016/j.engstruct.2009.02.017.
[25] Alipour A, Shafei B, Shinozuka M. Performance evaluation of deteriorating highway bridges located in high seismic areas. J Bridge Eng 2011;16. https://doi.org/10.1061/(asce)be.1943-5592.0000197.
[26] Avşar Ö, Yakut A, Caner A. Analytical fragility curves for ordinary highway bridges in Turkey. Earthq Spectra 2011;27. https://doi.org/10.1193/1.3651349.
[27] Borzi B, Ceresa P, Franchin P, Noto F, Calvi GM, Pinto PE. Seismic vulnerability of the Italian roadway bridge stock. Earthq Spectra 2015;31. https://doi.org/10.1193/070413EQS190M.
[28] Moschonas IF, Kappos AJ, Panetsos P, Papadopoulos V, Makarios T, Thanopoulos P. Seismic fragility curves for greek bridges: methodology and case studies. Bull Earthq Eng 2009;7. https://doi.org/10.1007/s10518-008-9077-2.
[29] Perdomo C, Monteiro R, Sucuoğlu H. Development of fragility curves for single-column RC italian bridges using nonlinear static analysis. J Earthq Eng 2022;26. https://doi.org/10.1080/13632469.2020.1760153.
[30] Cardone D, Perrone G, Sofia S. A performance-based adaptive methodology for the seismic evaluation of multi-span simply supported deck bridges. Bull Earthq Eng 2011;9. https://doi.org/10.1007/s10518-011-9260-8.
[31] Miano A, Jalayer F, De Risi R, Prota A, Manfredi G. Model updating and seismic loss assessment for a portfolio of bridges. Bull Earthq Eng 2016;14. https://doi.org/10.1007/s10518-015-9850-y.
[32] Eurocode Cen. Eurocode 8: Design of structures for earthquake resistance—Part 1: General rules, seismic actions and rules for buildings (EN 1998-1: 2004). European Committee for Normalization, Brussels 2004.
[33] D'Ayala D, Meslem A, Vamvatsikos D, Porter K, Rossetto T, Silva V. Guidelines for analytical vulnerability assessment of low/mid-rise buildings, vulnerability global component project. GEM Tech Rep 2015. -08 v100 2015;08.
[34] Porter K, Kennedy R, Bachman R. Creating fragility functions for performance-based earthquake engineering. Earthq Spectra 2007;23. https://doi.org/10.1193/1.2720892.
[35] Pagni CA, Lowes LN. Fragility functions for older reinforced concrete beam-column joints. Earthq Spectra 2006;22. https://doi.org/10.1193/1.2163365.
[36] Jeon JS, Lowes LN, DesRoches R, Brilakis I. Fragility curves for non-ductile reinforced concrete frames that exhibit different component response mechanisms. Eng Struct 2015;85. https://doi.org/10.1016/j.engstruct.2014.12.009.

[37] Federal Emergency Management Agency (FEMA). HAZUS-MH MR4 Technical Manual. National Institute of Building Sciences and Federal Emergency Management Agency (NIBS and FEMA) 2003.
[38] Cornell CA, Jalayer F, Hamburger RO, Foutch DA. Probabilistic basis for 2000 SAC federal emergency management agency steel moment frame guidelines. J Struct Eng 2002;128. https://doi.org/10.1061/(asce)0733-9445(2002)128:4(526).
[39] Crespi P, Zucca M, Longarini N, Giordano N. Seismic assessment of six typologies of existing RC bridges. Infrastructures 2020;5. https://doi.org/10.3390/INFRASTRUCTURES5060052.
[40] Crespi P, Zucca M, Valente M. On the collapse evaluation of existing RC bridges exposed to corrosion under horizontal loads. Eng Fail Anal 2020;116. https://doi.org/10.1016/j.engfailanal.2020.104727.
[41] Chopra AK, Goel RK. A modal pushover analysis procedure to estimate seismic demands for unsymmetric-plan buildings. Earthq Eng Struct Dyn 2004;33:903–27. https://doi.org/10.1002/EQE.380.
[42] Chopra AK, Goel RK. A modal pushover analysis procedure for estimating seismic demands for buildings. Earthq Eng Struct Dyn 2002;31:561–82. https://doi.org/10.1002/EQE.144.
[43] Paraskeva TS, Kappos AJ. Further development of a multimodal pushover analysis procedure for seismic assessment of bridges. Earthq Eng Struct Dyn 2010;39:211–22. https://doi.org/10.1002/EQE.947.
[44] Paraskeva TS, Kappos AJ, Sextos AG. Extension of modal pushover analysis to seismic assessment of bridges. Earthq Eng Struct Dyn 2006;35:1269–93. https://doi.org/10.1002/EQE.582.
[45] Department of Homeland Security. FEMA 440: Improvement of nonlinear static seismic analysis procedures. 2005.
[46] Appl Technol Counc ATC 40 Seism Eval Retrofit Concr Build 1996;1.
[47] Crespi P, Zucca M, Valente M, Longarini N. Influence of corrosion effects on the seismic capacity of existing RC bridges. Eng Fail Anal 2022;140. https://doi.org/10.1016/j.engfailanal.2022.106546.
[48] Zucca M, Crespi P, Stochino F, Puppio ML, Mistretta F, Longarini N, et al. Evaluation of maintenances intervention period on stock of existing RC bridges subject to damage phenomena. COMPDYN Proc 2023. https://doi.org/10.7712/120123.10627.20209.
[49] Federal Emergency Management Agency. Hazus 99 - Estimated Annualized Earthquake Losses for the United States. 2008.
[50] Pinho R, Monteiro R, Casarotti C, Delgado R. Assessment of continuous span bridges through nonlinear static procedures. Earthq Spectra 2009;25. https://doi.org/10.1193/1.3050449.
[51] Basöz NI, Kiremidjian AS, King SA, Law KH. Statistical analysis of bridge damage data from the 1994 Northridge, CA, earthquake. Earthq Spectra 1999;15. https://doi.org/10.1193/1.1586027.